MOVING SPRAY-PLATE CENTER-PIVOT SPRINKLER RATING INDEX FOR ASSESSING RUNOFF POTENTIAL

B. A. King

A Tribute to the Career of Terry Howell, Sr.

ABSTRACT. *Numerous moving spray-plate center-pivot sprinklers are commercially available, providing a range of droplet size distributions and wetted diameters. Currently lacking is a means to quantitatively compare sprinkler choices with regard to maximizing infiltration and minimizing runoff. The objective of this study was to develop a soil-independent, quantitative potential runoff index to facilitate selection of sprinklers for center-pivot sprinkler irrigation systems. Droplet sizes, droplet velocities, and water application rates of numerous moving spray-plate sprinklers were measured in the laboratory throughout a range of flow rates and operating pressures. The proposed sprinkler runoff index was based on application rates of kinetic energy and water computed by overlapping specific power and water application profiles of sprinklers equally spaced 3 m along a center-pivot lateral. Results show that substantial differences in runoff potential exist between sprinkler choices, and several sprinklers can have similar runoff potential index values. In some cases, equivalent potential runoff index values were obtained with compensating differences in specific power and application rate. The proposed sprinkler runoff index, in which larger index values reveal a lower potential for runoff, provides a new and unique approach for evaluating moving spray-plate sprinklers with regard to potential runoff. The runoff index provides an effective means for comparing sprinkler choices by identifying sprinklers with large droplets and relatively small wetted diameters.*

Keywords. Center-pivot, Infiltration, Kinetic energy, Runoff, Sprinkler, Sprinkler irrigation.

C enter-pivot and lateral-move (mechanical-move) irrigation systems were introduced over fifty years ago and now account for more than 80% of the sprinkler-irrigated area and more than 50% of the total irrigated area in the U.S. (USDA, 2014). The growth and popularity of these irrigation systems today is due to their high application uniformity when designed and managed properly, low labor requirement, and high degree of automation with mobile remote monitoring and control capability. Use of mechanical-move irrigation systems is likely to increase due to replacement of higher labor requirement set-move sprinkler irrigation systems, surface irrigation systems in response to limited water availability and adverse environmental impacts, and increased use in rainfed agriculture to reduce risk of drought at critical crop growth stages due to increasing climate variability. Runoff can be problematic with center-pivot irrigation systems, especially along the outer extent of the system lateral, where the application rate commonly exceeds the soil infil-

tration rate (Allen, 1990; Undersander et al., 1985; DeBoer et al., 1992; Ben-Hur et al., 1995; Kincaid, 2005; Silva, 2006; King and Bjorneberg, 2011). While runoff is a well-recognized problem, it is normally unseen because runoff often infiltrates before exiting the field boundary, as only a small fraction of the field is irrigated (saturated) at a given time and/or runoff collects in low spots within the field, resulting in non-uniform infiltration and variability in crop yield. Minimizing the application rate minimizes potential runoff, erosion, and non-uniform infiltration.

A drastic reduction in water infiltration rate is generally observed due to formation of a seal on the soil surface when discrete water droplets impact a bare soil surface (Duley, 1939; Borst and Woodburn, 1942; Ellison, 1945). McIntyre (1958) found that the saturated hydraulic conductivity of soil surface seal was two to three orders of magnitude less than that of underlying soil. The effect of soil surface seal formation on water infiltration rate has been studied by Agassi et al. (1985, 1994), Thompson and James (1985), Mohammed and Kohl (1987), Ben-Hur et al. (1987), Betzalel et al. (1995), and Assouline and Mualem (1997). These studies have shown that the kinetic energy of discrete droplets impacting a bare soil surface is a primary factor in determining the reduction in water infiltration rate due to soil surface seal formation. Much of the research on soil surface sealing has focused on rainfall conditions, but the same processes occur under sprinkler irrigation (von Bernuth and Gilley, 1985; Ben-Hur et al., 1995; DeBoer and Chu, 2001; Silva, 2006). King and Bjorneberg (2011)

Transactions of the ASABE

Vol. 59(1): 225-237   2016 American Society of Agricultural and Biological Engineers   ISSN 2151-0032   DOI 10.13031/trans.59.11162   225

observed significant differences in runoff and erosion between sprinkler types even though flow rates and wetted diameters were very similar. These observed differences highlight the effect that droplet kinetic energy can have on infiltration and runoff and that application rate alone is not necessarily a predictor of potential runoff. King and Bjorneberg (2012a) developed a transient sealing soil infiltration model that expressed infiltration rate as a function of droplet specific power (kinetic energy times application rate) that provided a good fit to rainfall infiltrometer data. Soil surface seal formation in combination with high water application rates under center-pivot sprinkler irrigation exacerbates potential runoff and erosion hazards. Sprinklers that minimize the rates at which kinetic energy and water are applied to the soil will minimize the potential for runoff under mechanical-move irrigation.

The influence that droplet kinetic energy applied by center-pivot sprinklers has on infiltration, runoff, and erosion is well known in the center-pivot sprinkler irrigation industry. Over the past three decades, center-pivot sprinkler manufacturers have continued to develop sprinklers that reduce peak water application rates and droplet kinetic energy to sustain infiltration rates and reduce runoff and erosion. Consequently, numerous sprinkler choices are available to the center-pivot irrigation system designer and crop producer; however, limited quantitative information is available that relates these choices to performance with regard to infiltration, runoff, and erosion. Sprinkler manufacturers do not provide quantitative information on sprinkler droplet size distribution or application rate profiles, precluding quantitative analysis in selecting mechanical-move irrigation system sprinklers. Kincaid (1996) developed a model to estimate sprinkler droplet kinetic energy per unit discharge volume of common sprinkler types as a function of nozzle size and operating pressure for use as a design aid in selecting center-pivot sprinklers. King and Bjorneberg (2010) evaluated droplet kinetic energy applied to the soil by moving spray-plate sprinklers and found that sprinkler droplet kinetic energy per unit discharge does not represent the actual droplet kinetic energy applied by center-pivot irrigation. King and Bjorneberg (2012b) evaluated several center-pivot sprinklers and found that droplet kinetic energy for a given flow rate and operating pressure varied by up to 200% among sprinklers. They concluded that the sprinkler with the lowest droplet kinetic energy or lowest specific power may not necessarily result in the greatest infiltrated depth or least runoff and erosion, which means that droplet kinetic energy is not suitable as a single parameter to select between sprinkler choices.

The objective of this study was to investigate development of a soil-independent, quantitative runoff potential index to facilitate selection of moving spray-plate sprinklers for mechanical-move sprinkler irrigation systems. A second objective was to apply the proposed index to numerous commercial center-pivot sprinklers based on measurement of sprinkler droplet sizes, droplet velocities, and application rate profiles in the laboratory over a range of flow rates and pressures. A third objective is to use the index to demonstrate differences in sprinkler characteristics with regard to potential infiltration and runoff with mechanical-move irrigation systems.

METHODS AND MATERIALS

Sprinkler devices and characteristics used in this study along with corresponding operating pressures, nozzle sizes, and flow rates are listed in table 1. The I-Wob, Xi-Wob (Senninger Irrigation, Inc., Clermont, Fla.), N3000, and O3000 (Nelson Irrigation Corp., Walla Walla, Wash.) sprinklers use an off-center oscillating plate with grooves of equal geometry to break up the nozzle jet and create discrete water droplets. The R3000 sprinklers (Nelson Irrigation Corp.) use a rotating plate with grooves to break up the

Table 1. Sprinkler types, nozzle sizes, pressures, and flow rates used in study (flow rates based on manufacturer data).

Nozzle Diameter (mm)	Flow Rate (L min^{-1}) at:			
	41 kPa	69 kPa	103 kPa	138 kPa
Senninger I-Wob: Black plate (9-groove standard angle), Blue plate (9-groove low angle), and White plate (6-groove low angle)				
3.57	-	6.9	8.2	9.5
5.56	-	16.6	19.8	22.8
7.94	-	33.1	39.5	45.6
Senninger I-Wob: Gray plate (6-groove low angle UP3 nozzle)				
3.57	-	6.9	8.4	9.7
5.56	-	16.7	20.5	23.7
7.94	-	34.1	41.8	48.3
Senninger Xi-Wob: Black plate (6-groove 15° trajectory), Blue plate (6-groove 10° trajectory), and Gray plate (9-groove 10° trajectory)				
3.57	-	6.9	8.2	-
5.56	-	16.6	19.8	-
7.94	-	33.1	39.5	-
Senninger Xi-Wob 605: White plate top-mount (6-groove 5° trajectory UP3 nozzle)				
4.17	-	9.3	-	-
6.35	-	21.9	-	-
8.93	-	43.0	-	-
Nelson N3000: Green plate (9-groove 21° trajectory) and Blue plate (7-groove 12° trajectory)				
3.77	-	7.5	9.1	-
5.75	-	17.5	21.4	-
8.14	-	35.5	43.5	-
Nelson O3000: Black plate (9-groove standard single trajectory)				
3.77	-	7.5	9.1	10.6
5.75	-	17.5	21.4	24.7
8.14	-	35.5	43.5	50.2
Nelson O3000: Purple plate (18-groove)				
3.77	-	-	9.1	-
5.75	-	-	21.4	-
8.14	-	35.5	43.5	50.2
Nelson S3000: Purple plate (6-groove multi-trajectory), Yellow plate (8-groove multi-trajectory), and Red plate (6-groove 12° trajectory)				
3.77	-	7.5	9.1	10.6
5.75	-	17.5	21.4	24.7
8.14	-	35.5	43.5	50.2
Nelson R3000: Red plate (6-groove 12° trajectory), Brown plate (6-groove multi-trajectory), Orange plate (8-groove multi-trajectory), and White plate top-mount (6-groove multi-trajectory)				
3.57	-	-	8.1	9.4
5.36	-	-	18.4	21.2
7.54	-	-	37.0	42.7
Nelson R3000: Blue plate top-mount (4-groove 8° trajectory)				
3.57	-	-	-	9.4
5.36	-	-	-	21.2
7.54	-	-	-	42.7
Nelson A3000: Maroon plate (4-groove multi-trajectory) and Gold plate (8-groove multi-trajectory)				
4.17	-	9.0	11.0	-
6.35	-	21.3	26.7	-
8.93	-	42.7	52.2	-
Nelson A3000: Navy plate top-mount (8-groove multi-trajectory)				
4.17	7.0	9.0	11.0	-
6.35	16.5	21.3	26.1	-
8.93	33.0	42.7	52.2	-

nozzle jet and create discrete streams of water leaving the plate edge. The difference between the various R3000 sprinkler plates is the number of grooves either of equal geometry or with multiple trajectory angles and widths (table 1), which affects the droplet sizes formed and their trajectory. The R3000 sprinklers have plate rotational speeds of 2 to 4 rpm. The S3000 sprinkler (Nelson Irrigation Corp.) also uses a rotating plate with grooves to break up the nozzle jet. The difference between the various S3000 sprinkler plates is also the number of grooves either of equal geometry or with multiple trajectory angles and widths (table 1). The S3000 sprinklers have rotational speeds of 400 to 500 rpm and are frequently termed spinning plate sprinklers. The A3000 sprinkler is similar in design to the R3000 and S3000 sprinklers with the main difference being plate geometry (table 1) and rotational speed dependent on flow rate and ranging between the speeds of the R3000 and S3000 sprinklers. Four sprinklers used in the study were designed to be mounted on top of an irrigation system lateral: R3000 blue plate, R3000 white plate, A3000 navy plate, and Senninger Xi-Wob white plate. Three flow rates were evaluated for each sprinkler: low (<12 L min⁻¹), medium (~20 L min⁻¹), and high (~45 L min⁻¹). Sprinkler nozzle sizes were selected to provide similar flow rates at the given operating pressures based on manufacturer data. Three operating pressures (69, 103, and 138 kPa) were evaluated for each sprinkler when within the manufacturer's recommended operating pressure. The A3000 navy plate sprinkler was also evaluated at 41 kPa operating pressure. Some of the tests were below the manufacturer's recommended design flow rates (I-Wob white plate) but were used regardless to maintain flow rate consistency across all sprinklers. This study spanned a seven-year period starting in 2009 and ongoing into 2015. Some of the sprinklers tested are no longer in production (N3000), and others have been modified with regard to nozzle mounting and flow rate (Senninger UP3 nozzle), but plate designs, to the author's knowledge, remained the same.

Droplet sizes and velocities were measured using a Thies Clima Laser Precipitation Monitor (TCLPM, Adolf Thies GmbH & Co. KG, Gottingen, Germany) (King et al., 2010). Measurements were conducted indoors at an air temperature and relative humidity of approximately 16°C and 49%, respectively, with no wind. The TCLPM measures droplet sizes from 0.16 to 8.0 mm. Droplet size measurements were grouped into 0.1 mm increments (±0.05 mm) for analysis, starting with 0.25 mm and continuing to 7.95 mm. Measured droplets less than 0.2 mm in diameter were discarded as they represented less than 0.05% of the total volume of droplets measured. The sprinkler was enclosed in a plastic cylinder similar to that described by Chen and Wallender (1985), with a lateral cutout that allowed a wedge-shaped portion of the sprinkler circular wetted area to be sampled. The interior of the enclosure was lined with aluminum honeycomb-type material 38 mm thick to minimize splash from the sprinkler jet impacting sides of the enclosure interfering with the sprinkler nozzle jet or its mechanical operation. The vertical edges of the enclosure cutout were fitted with metal strips with sharp edges angled inward to the vertical axis of the sprinkler to minimize splash from the sprinkler jet on the edge of the opening interfering with the nozzle jet as it exited the enclosure. Droplet size and velocity measurements were collected at 1 m increments radially outward from the sprinkler, with a 0.5 m radial increment used at the end of the wetted radius when necessary. A minimum of 10,000 droplets were measured at each location except at the most distal radial location or at intermediate radial locations where the application rate was less than 4 mm h⁻¹. At those locations, a minimum of 4,000 droplets were measured to reduce measurement time. Sprinklers designed for mounting below the irrigation system lateral were positioned on the end of a drop tube with the nozzle discharge directed vertically downward. The elevation difference between the sprinkler plate and laser beam of the TCLPM was 0.8 m. For sprinklers designed for mounting above the system lateral, the elevation difference between the sprinkler plate and laser beam of the TCLPM was 3.7 m. Pressure regulators with nominal pressure ratings for the test conditions were used to control pressure at the base of the sprinkler. A pressure gauge located upstream of the pressure regulator was used to monitor water supply pressure. Water supply pressures exceeded the nominal pressure rating of the regulator by a minimum of 69 kPa. The pressure between the pressure regulator and sprinkler was periodically checked to make sure it was within ±10 kPa of nominal pressure rating. Additional details of the experimental methods are provided by King et al. (2010).

Average radial application rate profiles for the sprinklers were also measured indoors with no wind. Catch cans, 150 mm in diameter and 180 mm tall, spaced at 0.5 m increments from the sprinkler in one radial direction, were used to collect water. Sprinklers designed for mounting below a system lateral were located 0.8 m above the can opening, and sprinklers designed for mounting above a system lateral were located 3.7 m above the can opening. The duration of each test was 30 to 60 min. Water volume collected in each can was measured using a graduated cylinder. Average application rate in each catch can was calculated by dividing the volume caught by the area of catch can entrance and the duration of each test.

Kinetic energy per unit sprinkler discharge, KE_{di} (J L⁻¹), at the ith radial location for each sprinkler was computed as (King and Bjorneberg, 2010):

$$KE_{di} = \frac{\sum_{j=1}^{ND_i} \frac{\rho_w \pi D_j^3 V_j^2}{12}}{1000 \sum_{j=1}^{ND_i} \frac{\pi D_j^3}{6}} \tag{1}$$

where ND_i is the number of droplets measured at the ith radial location, ρ_w is the mass density of water (kg m⁻³), D_j is the measured diameter (m) of the jth droplet, and V_j is the measured velocity (m s⁻¹) of the jth droplet. The resulting value represents the average kinetic energy per liter of droplet volume applied at the ith radial measurement location.

Specific power (SP, W m^{-2}), at the ith radial location was computed for each sprinkler as (King and Bjorneberg, 2010):

$$SP_i = KE_{di} \cdot \frac{AR_i}{3600} \qquad (2)$$

where AR$_i$ is the average application rate (mm h^{-1}) associated with the ith radial location. SP represents the rate at which kinetic energy is transferred to the soil surface as a function of radial distance from the sprinkler. A sprinkler radial SP distribution is analogous to a sprinkler radial water application rate distribution.

A model written in Visual Basic was used to simulate the composite water application rate for a 0.3 m spaced square grid oriented both perpendicular to and parallel to the lateral. The composite application rate was computed by overlapping the radial water application rate profiles from successive sprinklers spaced at 3 m increments along a system lateral (fig. 1). An average composite application rate distribution perpendicular to the sprinkler lateral was computed as the average of simulated application rates over a 3 m distance parallel to the system lateral between adjacent sprinklers (fig. 2). Sprinkler application rate profiles
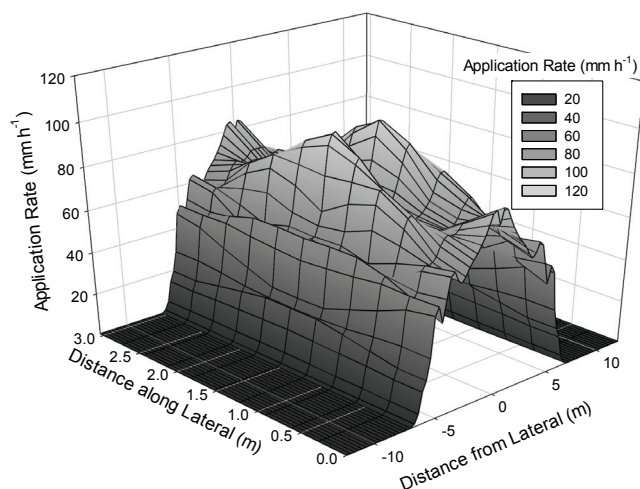

Figure 1. Composite water application pattern for an R3000 red plate sprinkler with 7.54 mm nozzle and 138 kPa operating pressure spaced 3 m along system lateral. Sprinklers are located at coordinates (0,0) and (0,3).
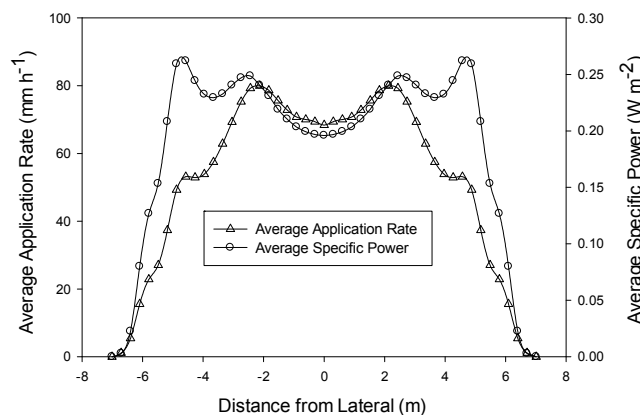

Figure 2. Average composite water application rate perpendicular to system lateral for an R3000 red plate sprinkler with 7.54 mm nozzle and 138 kPa operating pressure spaced 3 m along system lateral.

determined indoors were used in the simulation model. Sprinkler application rate profiles were interpolated to 0.3 m radial increments using cubic spline interpolation between catch can measurements. Average water application rate (AAR) was calculated as the arithmetic average of the average composite application rate distribution (fig. 2) perpendicular to the sprinkler lateral.

The composite SP distribution perpendicular to the center-pivot lateral was computed for each sprinkler using the sprinkler overap simulation model as the sum of SP from sprinklers applying water to a fixed point on the soil as the center-pivot system travels over the fixed point. Sprinkler SP distributions (eq. 2) were interpolated to 0.3 m radial distance increments using cubic spline interpolation. An average composite SP distribution was calculated as the average of simulated SP over a 3 m distance parallel to the center-pivot lateral centered about a sprinkler (fig. 2). Average SP (ASP) was calculated as the arithmetic average of the average composite SP distribution (fig. 2) perpendicular to the sprinkler lateral.

Water application rate relative to infiltration rate is a key parameter in determining runoff under center-pivot irrigation. When cumulative water application exceeds cumulative infiltration by a volume greater than soil surface storage, runoff is likely, resulting in non-uniform water application and erosion. Prediction of field infiltration rate is difficult at best; however, sprinklers with greater AAR have a greater potential for creating runoff. Soil surface seal formation has been shown to have a significant effect on infiltration rate of soils susceptible to sealing under droplet impact. King and Bjorneberg (2012a) found that transient infiltration rate of sealing soils could be modeled as a function of droplet specific power, where greater specific power results in lower infiltration rate. Thus, sprinklers with greater ASP will decrease infiltration rate of sealing soils, increasing the potential for runoff. Since greater AAR and ASP both increase the potential for runoff under sprinkler irrigation, it is logical to use these two parameters as a basis for selecting a sprinkler to minimize potential runoff. Based on this logic, a runoff index (RI) incorporating these two parameters was proposed. The index was calculated as:

$$RI = \frac{1}{AAR \cdot ASP} \qquad (3)$$

where AAR has units of mm h^{-1} and ASP has units of W m^{-2}, resulting in units of h m^2 mm^{-1} W^{-1} for RI. A greater RI value indicates a lower potential for runoff. Sprinklers used in this study included a large range of flow rates, leading to a large range in RI and precluded direct overall comparison of sprinklers across flow rates and pressures because AAR and ASP are flow rate dependent. In practice, selection of sprinkler operating pressure is primarily determined by energy cost and field topography, while sprinkler flow rate is primarily determined by system lateral location and peak crop evapotranspiration rate or available water supply. Therefore, equation 3 was modified to normalize AAR and ASP for small differences in flow rate between sprinklers having similar flow rates and equivalent operating pressures by dividing AAR (normalizing) by sprinkler flow rate and multiplying

by group mean flow rate. The resulting group runoff index (RI_g) was calculated as:

$$RI_g = \frac{1}{\text{AAR} \cdot \text{ASP}} \cdot \left(\frac{Q_s}{Q_m} \right)^2 \tag{4}$$

where Q_m is mean sprinkler flow rate (L min^{-1}) of sprinklers grouped by flow rate and operating pressure, and Q_s is sprinkler flow rate (L min^{-1}). Normalizing equation 3 for small differences in sprinkler flow rate allows direct comparison of RI_g values between sprinklers grouped by flow rate and operating pressure. Implicit in equation 4 are the assumptions that (1) sprinkler application rate at each radial location is a direct function of sprinkler flow rate, and (2) changes in droplet size and velocity are negligible for small changes in sprinkler flow rate, which are reasonable assumptions (data not shown).

Sprinklers used in the study were sorted by operating pressure and nozzle size. The resulting list was divided into groups according to pressure and low, medium, and high flow rate. The mean flow rate of each group (Q_m) was used in equation 4 to calculate RI_g for each sprinkler in a group. Sprinklers designed for mounting below and above an irrigation system lateral were analyzed separately.

Sprinkler wetted radius has a substantial effect on RI_g as AAR is indirectly related to wetted radius. For a given sprinkler flow rate, increasing wetted radius decreases AAR and increases RI_g. However, sprinklers with a larger wetted radius generally have larger droplet sizes, reducing the influence of wetted radius on decreasing ASP. In this study, droplet size, droplet velocity, and application rate profiles were measured using a sprinkler height of 0.8 m above the measuring device. Sprinkler wetted radius generally increases with mounting height; thus, RI_g values in this study would be greater had measurements been collected using a greater sprinkler height, and relative differences may have been less for sprinklers with low droplet trajectory angles. The 0.8 m measurement height was used in this study to include data collected from previous studies of sprinkler characteristics (King and Bjorneberg, 2012b) and field studies of sprinkler runoff (King and Bjorneberg, 2011) that used a 0.8 m mounting height.

To evaluate the applicability of RI_g for indicating relative potential runoff between sprinklers, sealing soil infiltration was estimated using the model developed by King and Bjorneberg (2012a). The model used a finite difference solution of Richard's infiltration equation that incorporated the effect of transient soil surface sealing on infiltration rate. The hydraulic conductivity of the soil surface seal, assumed to be 5 mm thick, was predicted as a function of cumulative droplet kinetic energy applied to the soil surface and soil-specific factors (King and Bjorneberg, 2012a). Hydraulic conductivity as a function of time was calculated as:

$$K(t) = K_f + \frac{(K_i - K_f)}{1 + S_f \left(\int_0^T \text{SP}(t) \cdot t \right)^{1.2}} \tag{5}$$

where $K(t)$ is soil hydraulic conductivity (mm h^{-1}) at time step t (s), K_f is final satiated hydraulic conductivity (mm h^{-1}) of the soil surface seal after an extended period of droplet impact absent the effect of seal erosion, K_i is initial satiated hydraulic conductivity of the surface soil (mm h^{-1}), S_f is a dimensionless empirical soil factor that represents resistance to surface seal formation, $\text{SP}(t)$ is specific power of droplets (W m^{-2}) at time step t, and T is the duration of the irrigation event. Hydraulic conductivity of a soil surface seal, $K(t)$, was assumed to be a monotonic decreasing function with time and not to increase with a decrease in $\text{SP}(t)$ during an irrigation event, such as when an irrigation system passes over a soil location and irrigation application rate decreases. Thus, the maximum value of $\text{SP}(t)$ during an irrigation event determined $K(t)$ for all subsequent time steps.

To calibrate the infiltration model, laboratory rainfall simulator tests were conducted on a Portneuf silt loam soil with particle size fractions of 14% sand, 65% silt, and 21% clay. Rainfall was simulated on the soil packed in a box measuring 0.3 m wide, 0.45 m deep, and 1.0 m long and placed on a 5% slope. Discrete water droplets were formed using 225 coiled micro-tubing, 0.8 mm diameter, with flow rate controlled using an adjustable constant head reservoir (Ogden et al., 1997). Droplet spacing was 45 mm on a square grid pattern covering a rectangular area 0.4 m wide by 1.1 m long. Oscillating fans on all four sides of the infiltrometer were used to randomly move droplet impact location on the soil surface. The soil was air dried, sieved, and packed to a bulk density of 1.3 to 1.4 Mg m^{-1}. The rainfall simulator produced droplets with kinetic energies per unit volume of 3.9 and 8.5 J m^{-2} mm^{-1} using fall heights of 0.3 and 1.0 m, respectively. Zero kinetic energy water application was simulated by placing an evaporative cooler pad over a screen with 7.6 mm square opening suspended 20 mm above the soil surface. Water application rates ranged from 90 to 235 mm h^{-1}. Rainfall simulation duration ranged from 30 to 60 min. Runoff volume was measured by continuously recording the cumulative weight of runoff water. Total infiltrated volume was determined by weighing the soil box immediately before and after rainfall simulation. Water application rate was calculated by dividing the sum of infiltrated and runoff volumes by time of application. Infiltration rate was calculated as the difference between water application rate and runoff rate, neglecting soil surface storage. Specific power of the simulated rainfall was calculated as:

$$\text{SP} = \frac{\text{KE}_d \cdot R}{3600} \tag{6}$$

where KE_d is droplet kinetic energy per unit volume (J m^{-2} mm^{-1}), and R is application rate (mm h^{-1}).

Infiltration model goodness of fit was quantified by examining the sum of squared difference between model-predicted values and measured data relative to the sum of squared difference between the data and mean data value, which is termed model efficiency (ME). Model efficiency (Nash and Sutcliffe 1970) is defined as:

$$ME = 1 - \frac{\sum\left(y_i - y_{pred}\right)^2}{\sum\left(y_i - y_{avg}\right)^2} \qquad (7)$$

where y_i is the ith data value, y_{pred} is the model-predicted value for y_i, and y_{avg} is the mean of the data values. Model efficiency was used to optimize model parameters and quantify goodness of fit. Model efficiency is similar to the correlation coefficient associated with linear regression in that its value ranges from -∞ to 1. A value of 1 means the model is a perfect fit to the data, but a negative ME value signifies that the data mean is a better estimate of the data than the model. Use of ME alone can be misleading, as it does not take into account other factors that enter into determining model goodness of fit. For example, a reliable estimate of time to ponding is important for infiltration models but is not quantified by using ME alone. Model parameters were determined based on maximizing ME but adjusted when there was considerable variability in the data to provide an improved estimate of mean time to ponding with little quantitative decrease in the value of ME.

Soil water retention characteristics of Portneuf silt loam were estimated based on soil texture using the pedotransfer functions of Saxton and Rawls (2006). The Brooks and Corey (1964) relationships were used to model soil hydraulic properties as a function of soil water potential. Parameters for the Brooks and Corey (1964) soil water relationships were estimated by fitting them to values of soil water potential versus soil water content estimated by the Saxton and Rawls (2006) pedotransfer functions. Satiated water content was taken as 80% of pedotransfer function predicted porosity. Water entry pressure head for soil wetting was taken as one-third of the air entry pressure estimated by the Saxton and Rawls (2006) pedotransfer function. Values used to characterize soil water retention properties of Portneuf silt loam are given in table 2.

The three parameters used in modeling infiltration under transient soil surface seal development (eq. 5) were determined by fitting the infiltration model to laboratory infiltration data for Portneuf silt loam over the range of specific powers tested. The value for initial satiated hydraulic conductivity (K_i) for each soil was determined by trial-and-error fitting of the infiltration model to maximize ME when the soil surface was protected from droplet impact (fig. 3). The value obtained for K_i was held constant for all subsequent model simulations under transient soil seal development due to varying kinetic energy levels and application intensities (SP, eq. 6). The values for K_f and S_f were then determined jointly for each soil by trial-and-error fitting of
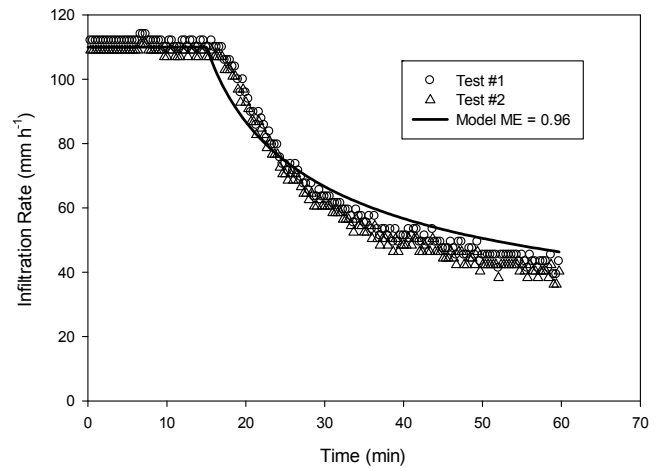

Figure 3. Infiltration model fit to infiltrometer data from protected soil surface conditions used to determine satiated hydraulic conductivity of Portneuf silt loam soil.

the two parameters to maximize ME for each specific power (fig. 4).

Model efficiency of the infiltration model for the rainfall infiltrometer data with four droplet SP values ranged from 0.84 to 0.91 (fig. 4). The value selected for S_f (eq. 5) was 0.06 and held constant for all SP. The value for K_f ranged from 0.15 to 0.03 mm h^{-1} depending on SP (fig. 5). The power equation relating K_f to SP (fig. 5) was used in the infiltration model to account for the variation in SP with time as a mechanical-move irrigation system passes over a soil location.

RESULTS AND DISCUSSION

Sprinkler flow rate, ASP, AAR, and RI$_g$ grouped by low, medium, and high flow rate along with group mean flow rate (Q_m) are given for sprinklers mounted below the irrigation system lateral and operating pressures of 69 kPa in table 3, 103 kPa in table 4, and 138 kPa in table 5. Values of RI$_g$ differed substantially between flow rate groups at a given operating pressure, demonstrating the need to group sprinklers by flow rate and limit comparisons to within a flow rate group. Normalizing RI$_g$ for differences within a flow rate grouping accounted for differences in ASP and AAR due to sprinkler flow rate differences. For example, at low flow and 69 kPa, RI$_g$ (table 3) and RI (not shown) were 2.52 and 2.91, respectively, for the I-Wob gray plate sprinkler, and RI$_g$ and RI (not shown) were 2.63 and 2.56, respectively, for the S3000 red plate sprinkler. The relative ranking of the runoff index was reversed (RI$_g$ versus RI) if differences in ASP and AAR due to sprinkler flow rate differences were not considered.

For an operating pressure of 69 kPa, RI$_g$ values for the low flow sprinkler group ranged from 1.65 to 3.13 (table 3). Recall that larger RI$_g$ values reveal a lower potential for runoff. The O3000 black plate sprinkler (RI$_g$ = 3.13) had the least and the A3000 maroon plate sprinkler (RI$_g$ = 1.65) had the greatest potential for runoff, and five sprinklers had RI$_g$ values greater than 2.50. The relatively large range in RI$_g$ values (1.9:1) indicates that differences in

Table 2. Soil hydraulic parameters used in the sealing soil infiltration model to predict infiltration under simulated rainfall for Portneuf silt loam soil.

Parameter	Value
Porosity	0.48
Residual moisture content (% volume)	2.4
Satiated moisture content (% volume)	38.6
Initial soil water potential (mm)	-50,000
Water entry head (mm)	-451
Brooks-Corey exponent (λ)	0.32
Satiated hydraulic conductivity (mm h^{-1})[a]	11.0

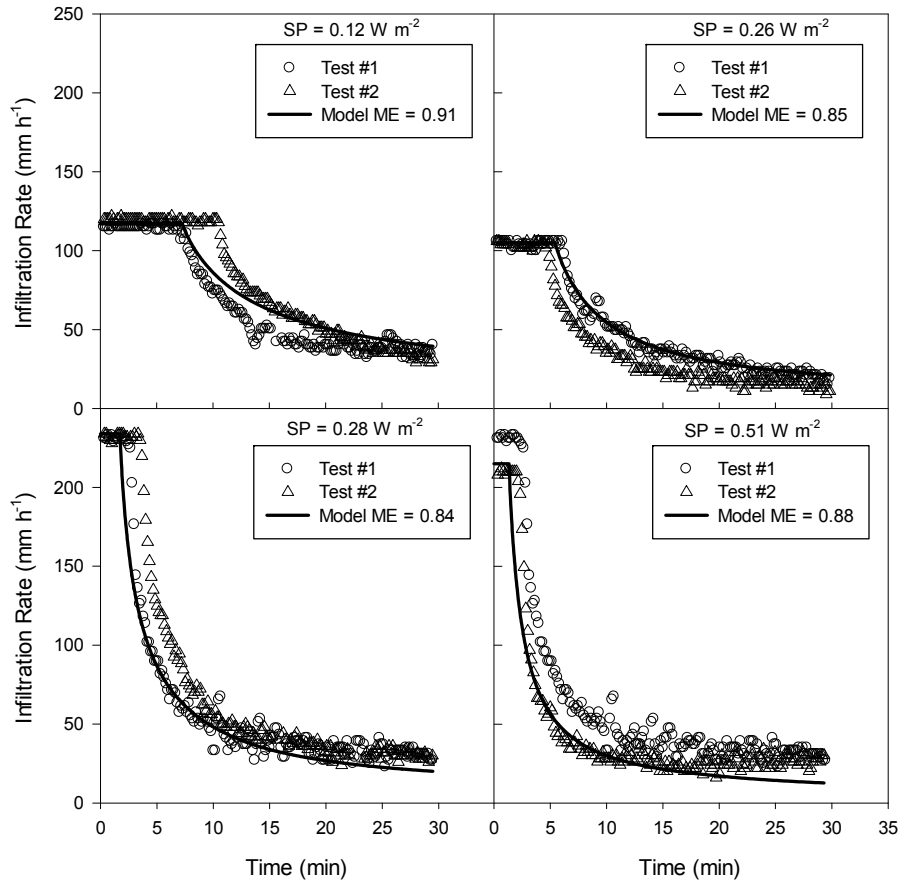[a] Equal to K_i in equation 5 for protected soil surface.

Figure 4. Infiltration model fit to infiltrometer data for four values of droplet specific power (SP) when calibrated for Portneuf silt loam soil.
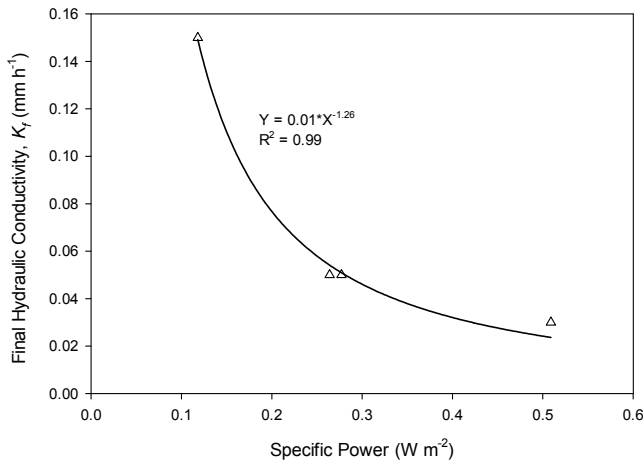

Figure 5. Relationship between specific power and final hydraulic conductivity of the soil surface seal used in the infiltration model calibrated for Portneuf silt loam soil.

sprinkler characteristics in terms of droplet size and wetted radius exist among the sprinklers. For the medium flow rate sprinklers, the S3000 red plate sprinkler had the minimum (RI_g = 0.26) and A3000 gold plate sprinkler had the maximum (RI_g = 0.65) RI_g value for an operating pressure of 69 kPa. Four sprinklers in this group had RI_g values greater than 0.50. The relative range in RI_g values (2.0:1) was similar to the low flow rate sprinklers. For the high flow rate sprinkler group with an operating pressure of 69 kPa, the A3000 maroon plate and I-Wob blue plate sprinklers had

the smallest (RI_g = 0.06) and the A3000 gold plate sprinkler had the largest (RI_g = 0.22) RI_g value. The relative range in RI_g values (3.7:1) was greatest for the high flow rate sprinkler group. Four sprinklers in the high flow rate group had RI_g values greater than 0.12.

For an operating pressure of 103 kPa, RI_g values for the low flow sprinkler group ranged from 1.92 to 3.92 (table 4), indicating the A3000 gold plate sprinkler had the smallest and the I-Wob blue plate sprinkler had the largest potential for runoff. Four sprinklers had RI_g values greater than 2.85. The relative range in RI_g values was 2.1:1, very similar to the value for the low flow sprinkler group at 69 kPa. For the medium flow rate sprinkler group with an operating pressure of 103 kPa, the A3000 gold plate sprinkler (RI_g = 0.82) had the smallest and the S3000 red plate sprinkler (RI_g = 0.28) had the greatest potential for runoff. The relative range in RI_g values was 2.9:1, similar to the low flow sprinkler group. For the high flow sprinkler group at 103 kPa, the O3000 purple plate sprinkler had the largest RI_g value (RI_g = 0.16) and the N3000 blue plate sprinkler with RI_g = 0.06 had the largest potential for runoff. The relative range in RI_g values was 2.7:1, and four sprinklers had RI_g values greater than 0.11.

For an operating pressure of 138 kPa, RI_g values for the low flow sprinkler group ranged from to 1.48 to 2.58 (table 5). The R3000 brown plate sprinkler had the smallest and the I-Wob blue plate sprinkler had the largest potential for runoff. The range in relative RI_g values was 1.7:1. For

Table 3. Nozzle size, flow rate, average specific power (ASP), average application rate (AAR), and group runoff index (RI$_g$) for sprinklers tested at 69 kPa operating pressure mounted below the irrigation system lateral at a height of 0.8 m above ground level and spaced 3 m along the lateral. Also given is the group mean flow rate.

Flow Rate	Nozzle	Size (mm)	Flow Rate (L min^{-1})	ASP (W m^{-2})	AAR (mm h^{-1})	RI$_g$ (h m^2 W^{-1} mm^{-1})
Low	Nelson A3000 Gold plate	4.17	9.0	0.053	15.2	1.83
	Nelson A3000 Maroon plate	4.17	9.0	0.058	15.4	1.65
	Nelson N3000 Blue plate	3.77	7.5	0.035	13.6	2.15
	Nelson N3000 Green plate	3.77	7.5	0.035	11.8	2.47
	Nelson O3000 Black plate	3.77	7.5	0.032	10.2	3.13
	Nelson S3000 Purple plate	3.77	7.5	0.032	13.5	2.37
	Nelson S3000 Red plate	3.77	7.5	0.026	15.0	2.63
	Nelson S3000 Yellow plate	3.77	7.5	0.032	12.8	2.51
	Senninger I-Wob Black plate	3.57	6.9	0.032	11.2	2.41
	Senninger I-Wob Blue plate	3.57	6.9	0.035	14.7	1.68
	Senninger I-Wob Gray plate	3.57	6.9	0.024	14.3	2.52
	Senninger I-Wob White plate	3.57	6.9	0.037	11.9	1.96
	Senninger Xi-Wob Black plate	3.57	6.9	0.030	13.3	2.17
	Senninger Xi-Wob Blue plate	3.57	6.9	0.029	14.9	2.00
	Senninger Xi-Wob Gray plate	3.57	6.9	0.025	13.0	2.66
	Group mean flow rate =		7.4			
Medium	Nelson A3000 Gold plate	6.35	21.3	0.079	28.5	0.65
	Nelson A3000 Maroon plate	6.35	21.3	0.117	40.1	0.31
	Nelson N3000 Blue plate	5.75	17.5	0.084	31.0	0.38
	Nelson N3000 Green plate	5.75	17.5	0.070	26.5	0.53
	Nelson O3000 Black plate	5.75	17.5	0.075	22.7	0.58
	Nelson S3000 Purple plate	5.75	17.5	0.089	29.0	0.38
	Nelson S3000 Red plate	5.75	17.5	0.107	36.3	0.26
	Nelson S3000 Yellow plate	5.75	17.5	0.086	34.3	0.34
	Senninger I-Wob Black plate	5.56	16.6	0.067	26.1	0.51
	Senninger I-Wob Blue plate	5.56	16.6	0.093	28.7	0.33
	Senninger I-Wob Gray plate	5.56	16.7	0.066	34.8	0.39
	Senninger I-Wob White plate	5.56	16.6	0.101	28.7	0.31
	Senninger Xi-Wob Black plate	5.56	16.6	0.074	28.2	0.43
	Senninger Xi-Wob Blue plate	5.56	16.6	0.082	30.7	0.35
	Senninger Xi-Wob Gray plate	5.56	16.6	0.087	30.7	0.33
	Group mean flow rate =		17.6			
High	Nelson A3000 Gold plate	8.93	42.7	0.120	54.5	0.22
	Nelson A3000 Maroon plate	8.93	42.7	0.312	80.9	0.06
	Nelson N3000 Blue plate	8.14	35.5	0.202	60.0	0.08
	Nelson N3000 Green plate	8.14	35.5	0.156	50.7	0.13
	Nelson O3000 Black plate	8.14	35.5	0.185	51.7	0.11
	Nelson O3000 Purple plate	8.14	35.5	0.157	51.4	0.12
	Nelson S3000 Purple plate	8.14	35.5	0.188	54.2	0.10
	Nelson S3000 Red plate	8.14	35.5	0.192	65.5	0.08
	Nelson S3000 Yellow plate	8.14	35.5	0.232	61.4	0.07
	Senninger I-Wob Black plate	7.94	33.1	0.146	47.2	0.13
	Senninger I-Wob Blue plate	7.94	33.1	0.244	57.9	0.06
	Senninger I-Wob Gray plate	7.94	34.1	0.129	57.4	0.13
	Senninger I-Wob White plate	7.94	33.1	0.237	54.4	0.07
	Senninger Xi-Wob Black plate	7.94	33.1	0.150	50.6	0.12
	Senninger Xi-Wob Blue plate	7.94	33.1	0.163	60.8	0.09
	Senninger Xi-Wob Gray plate	7.94	33.1	0.173	62.5	0.08
	Group mean flow rate =		35.4			

the medium flow rate sprinkler group with an operating pressure of 138 kPa, the I-Wob gray plate sprinkler (RI$_g$ = 0.49) had the smallest and the I-Wob blue plate sprinkler (RI$_g$ = 0.22) had the greatest potential for runoff. The range in relative RI$_g$ values was 2.2:1, similar to the low flow sprinkler group, and six sprinklers had RI$_g \geq 0.40$. For the high flow rate sprinkler group with an operating pressure of 138 kPa, the R3000 brown plate sprinkler (RI$_g$ = 0.13) had the smallest and the I-Wob blue plate sprinkler (RI$_g$ = 0.06) had the greatest potential for runoff. The relative range in RI$_g$ values was 2.2:1.

Flow rate, ASP, AAR, and RI$_g$ grouped by low, medium, and high flow rate along with group mean flow rate (Q_m) are given in table 6 for sprinklers mounted on top of the irrigation system lateral with operating pressures of 41,

69, 103, and 138 kPa. These sprinklers were analyzed separately from sprinklers mounted below the irrigation system lateral because the design decision to select top-mounted sprinklers is normally made for reasons such as crop interference rather than runoff potential. A limited number of moving-plate sprinklers are available for mounting above the system lateral; consequently, there are limited differences between sprinkler choices. For an operating pressure of 69 kPa, the Xi-Wob white plate sprinkler had the smallest (RI$_g$ = 2.94) runoff potential at the low flow rate, the A3000 navy plate sprinkler had the smallest (RI$_g$ = 0.46) runoff potential at the medium flow rate, and both sprinklers had equal runoff potential (RI$_g$ = 0.10) at the high flow rate. For an operating pressure of 103 kPa, the R3000 navy plate sprinkler provided the largest RI$_g$ value across

Table 4. Nozzle size, flow rate, average specific power (ASP), average application rate (AAR), and group runoff index (RI$_g$) for sprinklers tested at 103 kPa operating pressure mounted below the irrigation system lateral at a height of 0.8 m above ground level and spaced 3 m along the lateral. Also given is the group mean flow rate.

Flow Rate	Nozzle	Size (mm)	Flow Rate (L min^{-1})	ASP (W m^{-2})	AAR (mm h^{-1})	RI$_g$ (h m^2 W^{-1} mm^{-1})
Low	Nelson A3000 Gold plate	4.17	11.0	0.031	12.8	3.92
	Nelson A3000 Maroon plate	4.17	11.0	0.049	14.8	2.14
	Nelson N3000 Blue plate	3.77	9.1	0.030	16.5	2.15
	Nelson N3000 Green plate	3.77	9.1	0.030	12.4	2.86
	Nelson O3000 Black plate	3.77	9.1	0.029	11.8	3.11
	Nelson O3000 Purple plate	3.77	9.1	0.028	13.0	2.93
	Nelson R3000 Brown plate	3.57	8.1	0.029	12.2	2.35
	Nelson R3000 Orange plate	3.57	8.1	0.037	10.1	2.29
	Nelson R3000 Red plate	3.57	8.1	0.023	12.7	2.91
	Nelson S3000 Purple plate	3.77	9.1	0.030	15.2	2.31
	Nelson S3000 Red plate	3.77	9.1	0.031	15.5	2.26
	Nelson S3000 Yellow plate	3.77	9.1	0.030	13.1	2.76
	Senninger I-Wob Black plate	3.57	8.2	0.027	13.9	2.30
	Senninger I-Wob Blue plate	3.57	8.2	0.031	14.5	1.92
	Senninger I-Wob Gray plate	3.57	8.4	0.023	14.0	2.82
	Senninger I-Wob White plate	3.57	8.2	0.031	12.8	2.18
	Senninger Xi-Wob Black plate	3.57	8.2	0.026	14.7	2.26
	Senninger Xi-Wob Blue plate	3.57	8.2	0.029	13.5	2.21
	Senninger Xi-Wob Gray plate	3.57	8.2	0.028	15.0	2.06
	Group mean flow rate =		8.8			
Medium	Nelson A3000 Gold plate	6.35	26.1	0.065	29.4	0.82
	Nelson A3000 Maroon plate	6.35	26.1	0.105	34.8	0.43
	Nelson N3000 Blue plate	5.75	21.4	0.082	32.2	0.40
	Nelson N3000 Green plate	5.75	21.4	0.078	30.2	0.45
	Nelson O3000 Black plate	5.75	21.4	0.086	29.4	0.42
	Nelson O3000 Purple plate	5.75	21.4	0.069	31.5	0.48
	Nelson R3000 Brown plate	5.36	18.4	0.055	20.1	0.70
	Nelson R3000 Orange plate	5.36	18.4	0.066	21.7	0.54
	Nelson R3000 Red plate	5.36	18.4	0.071	24.1	0.46
	Nelson S3000 Purple plate	5.75	21.4	0.076	28.4	0.49
	Nelson S3000 Red plate	5.75	21.4	0.105	35.7	0.28
	Nelson S3000 Yellow plate	5.75	21.4	0.094	32.4	0.35
	Senninger I-Wob Black plate	5.56	19.8	0.065	28.0	0.49
	Senninger I-Wob Blue plate	5.56	19.8	0.090	31.7	0.32
	Senninger I-Wob Gray plate	5.56	20.5	0.056	30.6	0.56
	Senninger I-Wob White plate	5.56	19.8	0.095	28.4	0.33
	Senninger Xi-Wob Black plate	5.56	19.8	0.076	30.1	0.39
	Senninger Xi-Wob Blue plate	5.56	19.8	0.074	34.6	0.35
	Senninger Xi-Wob Gray plate	5.56	19.8	0.073	35.4	0.35
	Group mean flow rate =		20.9			
High	Nelson A3000 Gold plate	8.93	52.2	0.092	61.9	0.14
	Nelson A3000 Maroon plate	8.93	52.2	0.268	76.2	0.08
	Nelson N3000 Blue plate	8.14	43.5	0.230	74.4	0.06
	Nelson N3000 Green plate	8.14	43.5	0.168	60.7	0.11
	Nelson O3000 Black plate	8.14	43.5	0.230	58.7	0.08
	Nelson O3000 Purple plate	8.14	43.5	0.132	51.9	0.16
	Nelson R3000 Brown plate	7.54	37.0	0.145	51.4	0.10
	Nelson R3000 Orange plate	7.54	37.0	0.177	41.8	0.10
	Nelson R3000 Red plate	7.54	37.0	0.195	54.0	0.07
	Nelson S3000 Purple plate	8.14	43.5	0.188	61.7	0.09
	Nelson S3000 Red plate	8.14	43.5	0.163	64.4	0.10
	Nelson S3000 Yellow plate	8.14	43.5	0.211	61.5	0.08
	Senninger I-Wob Black plate	7.94	39.5	0.159	51.9	0.11
	Senninger I-Wob Blue plate	7.94	39.5	0.228	56.1	0.07
	Senninger I-Wob Gray plate	7.94	41.8	0.122	65.1	0.12
	Senninger I-Wob White plate	7.94	39.5	0.229	55.6	0.07
	Senninger Xi-Wob Black plate	7.94	39.5	0.130	54.3	0.13
	Senninger Xi-Wob Blue plate	7.94	39.5	0.149	62.9	0.09
	Senninger Xi-Wob Gray plate	7.94	39.5	0.161	66.5	0.08
	Group mean flow rate =		42.0			

all flow rates. For an operating pressure of 138 kPa, the R3000 white plate sprinkler had the largest RI$_g$ value for the low flow rate, but the R3000 blue plate sprinkler had the largest RI$_g$ value for the medium and high flow rates.

The proposed potential runoff index can also be used to compare sprinklers with different operating pressures but similar high flow rates. For example, RI$_g$ values for nine sprinklers (table 7) were compared across multiple operating pressures and ranged from 0.16 to 0.04. The R3000 brown plate sprinkler (RI$_g$ = 0.16) had the smallest and the A3000 Maroon plate sprinkler (RI$_g$ = 0.04) had the largest potential for runoff. The relative range in RI$_g$ values was

Table 5. Nozzle size, flow rate, average specific power (ASP), average application rate (AAR), and group runoff index (RI$_g$) for sprinklers tested at 138 kPa operating pressure mounted below the irrigation system lateral at a height of 0.8 m above ground level and spaced 3 m along the lateral. Also given is the group mean flow rate.

Flow Rate	Nozzle	Size (mm)	Flow Rate (L min^{-1})	ASP (W m^{-2})	AAR (mm h^{-1})	RI$_g$ (h m^2 W^{-1} mm^{-1})
Low	Nelson O3000 Black plate	3.77	10.6	0.039	14.6	2.02
	Nelson R3000 Brown plate	3.57	9.4	0.030	11.8	2.58
	Nelson R3000 Orange plate	3.57	9.4	0.040	12.0	1.88
	Nelson R3000 Red plate	3.57	9.4	0.027	16.2	2.06
	Nelson S3000 Purple plate	3.77	10.6	0.031	16.4	2.25
	Nelson S3000 Red plate	3.77	10.6	0.035	17.0	1.95
	Nelson S3000 Yellow plate	3.77	10.6	0.034	17.3	1.97
	Senninger I-Wob Black plate	3.57	9.5	0.025	14.5	2.54
	Senninger I-Wob Blue plate	3.57	9.5	0.035	17.8	1.48
	Senninger I-Wob Gray plate	3.57	9.7	0.024	17.8	2.25
	Senninger I-Wob White plate	3.57	9.5	0.034	14.7	1.85
	Group mean flow rate =		9.9			
Medium	Nelson O3000 Black plate	5.75	24.7	0.095	34.9	0.34
	Nelson R3000 Brown plate	5.36	21.2	0.069	29.1	0.42
	Nelson R3000 Orange plate	5.36	21.2	0.083	23.5	0.43
	Nelson R3000 Red plate	5.36	21.2	0.071	28.2	0.42
	Nelson S3000 Purple plate	5.75	24.7	0.073	33.0	0.47
	Nelson S3000 Red plate	5.75	24.7	0.081	44.0	0.32
	Nelson S3000 Yellow plate	5.75	24.7	0.087	41.7	0.32
	Senninger I-Wob Black plate	5.56	22.8	0.071	31.7	0.43
	Senninger I-Wob Blue plate	5.56	22.8	0.108	41.7	0.22
	Senninger I-Wob Gray plate	5.56	23.7	0.057	37.5	0.49
	Senninger I-Wob White plate	5.56	22.8	0.099	33.7	0.29
	Group mean flow rate =		23.1			
High	Nelson O3000 Black plate	8.14	50.2	0.183	70.0	0.09
	Nelson O3000 Purple plate	8.14	50.2	0.149	69.5	0.11
	Nelson R3000 Brown plate	7.54	42.7	0.129	47.6	0.13
	Nelson R3000 Orange plate	7.54	42.7	0.198	51.2	0.08
	Nelson R3000 Red plate	7.54	42.7	0.172	51.0	0.09
	Nelson S3000 Purple plate	8.14	50.2	0.170	68.3	0.10
	Nelson S3000 Red plate	8.14	50.2	0.185	74.3	0.08
	Nelson S3000 Yellow plate	8.14	50.2	0.222	73.3	0.07
	Senninger I-Wob Black plate	7.94	45.6	0.160	58.2	0.10
	Senninger I-Wob Blue plate	7.94	45.6	0.210	70.2	0.06
	Senninger I-Wob Gray plate	7.94	48.3	0.127	67.2	0.12
	Senninger I-Wob White plate	7.94	45.6	0.229	61.4	0.07
	Group mean flow rate =		47.0			

4.0:1, indicating substantial differences between sprinklers with regard to droplet sizes and application rates. Three sprinklers had RI$_g \geq 0.14$, indicating low potential for runoff: R3000 brown plate, A3000 gold plate, and O3000 purple plate. Model-predicted infiltration for 25.4 mm irrigation application on bare dry soil was greatest for these three sprinklers (table 7). The A3000 gold plate sprinkler had the greatest predicted infiltration (22.0 mm), followed by the R3000 brown plate sprinkler (21.0 mm) and the O3000 purple plate sprinkler (20.5 mm). Sprinklers with RI$_g > 0.14$ had the largest predicted infiltration depths, demonstrating that the proposed RI$_g$ value provides a good relative index of sprinkler runoff potential for a Portneuf silt loam soil. Predicted infiltration was greatest for the sprinkler with the smallest ASP rather than largest RI$_g$ value. This was due to the sensitivity of soil K_f to specific power (table 7), which is soil-dependent and not accounted for by the soil-independent RI$_g$ parameter.

In a field study of the R3000 brown plate, R3000 red plate, and S3000 purple plate sprinklers (table 7) on a Portneuf silt loam soil, King and Bjorneberg (2011) found that runoff for the S3000 purple plate sprinkler (RI$_g = 0.09$) was significantly greater than for the R3000 red plate (RI$_g = 0.11$) and R3000 brown plate (RI$_g = 0.16$) sprinklers and

found no significant differences in runoff between the R3000 brown plate and R3000 red plate sprinklers. From a practical point of view, differences in runoff of less than 15% are not likely measureable in the field, given the degree of variability often present with infiltration rate and soil surface storage. Therefore, with a Portneuf silt loam soil, runoff differences for sprinklers with RI$_g \geq 0.10$ are not likely measureable. The sensitivity of soil K_f in the range of sprinkler ASP affects the range of RI$_g$ values that represent a measureable difference in runoff. In general, differences in RI$_g$ values within 15% to 20% of the maximum value for high flow rate sprinklers would not likely have measureable runoff differences in the field.

The proposed sprinkler runoff index (RI$_g$) provides a means for comparing a group of moving spray-plate sprinklers design choices with regard to two main factors that affect potential runoff under mechanical-move irrigation systems. The results show that sprinkler plate configuration and mode of action can have a substantial effect on the rates of kinetic energy (ASP) and water (AAR) applied by mechanical-move irrigation systems. Sprinklers with equal RI$_g$ values can have substantially different ASP and AAR values, for example, the R3000 brown plate and A3000 gold plate sprinklers (table 7). Runoff from the two sprin-

Operating Pressure	Flow Rate	Nozzle	Size (mm)	Flow Rate (L min⁻¹)	ASP (W m⁻²)	AAR (mm h⁻¹)	RI_g (h m² W⁻¹ mm⁻¹)
41 kPa	Low	Nelson A3000 Navy plate	4.17	7.0	0.052	11.0	1.75
	Medium	Nelson A3000 Navy plate	6.35	16.5	0.163	24.4	0.25
	High	Nelson A3000 Navy plate	8.93	33.0	0.371	46.0	0.06
69 kPa	Low	Senninger Xi-Wob White plate	4.17	9.4	0.031	11.4	2.94
		Nelson A3000 Navy plate	4.17	9.0	0.041	8.9	2.64
		Group mean flow rate =		9.2			
	Medium	Senninger Xi-Wob White plate	6.35	21.2	0.098	27.3	0.37
		Nelson A3000 Navy plate	6.35	21.3	0.117	18.7	0.46
		Group mean flow rate =		21.3			
	High	Senninger Xi-Wob White plate	8.93	42.7	0.195	52.2	0.10
		Nelson A3000 Navy plate	8.93	42.7	0.229	43.8	0.10
		Group mean flow rate =		42.7			
103 kPa	Low	Nelson R3000 White plate	3.57	8.1	0.047	7.8	1.94
		Nelson A3000 Navy plate	4.17	11.0	0.034	8.7	4.55
		Group mean flow rate =		9.6			
	Medium	Nelson R3000 White plate	5.36	18.4	0.128	17.0	0.31
		Nelson A3000 Navy plate	6.35	26.1	0.130	26.3	0.40
		Group mean flow rate =		22.3			
	High	Nelson R3000 White plate	7.54	37.0	0.280	34.0	0.07
		Nelson A3000 Navy plate	8.93	52.2	0.206	51.0	0.13
		Group mean flow rate =		44.6			
138 kPa	Low	Nelson R3000 Blue plate	3.57	9.4	0.047	9.3	2.30
		Nelson R3000 White plate	3.57	9.4	0.033	8.3	3.63
		Group mean flow rate =		9.4			
	Medium	Nelson R3000 Blue plate	5.36	21.2	0.100	19.0	0.52
		Nelson R3000 White plate	5.36	21.2	0.115	20.3	0.43
		Group mean flow rate =		21.2			
	High	Nelson R3000 Blue plate	7.54	42.7	0.168	40.6	0.15
		Nelson R3000 White plate	7.54	42.7	0.186	37.3	0.14
		Group mean flow rate =		42.7			

Nozzle	Size (mm)	Pressure (kPa)	Flow Rate (L min⁻¹)	ASP (W m⁻²)	AAR (mm h⁻¹)	RI_g (h m² W⁻¹ mm⁻¹)	Model-Predicted Infiltration (mm)
Nelson A3000 Gold plate	8.93	69	42.7	0.120	54.5	0.15	22.0
Nelson A3000 Maroon plate	8.93	69	42.7	0.312	80.9	0.04	14.6
Nelson O3000 Black plate	8.14	103	43.5	0.230	58.7	0.08	18.3
Nelson O3000 Purple plate	8.14	103	43.5	0.132	51.9	0.15	20.5
Nelson R3000 Brown plate	7.54	138	42.7	0.129	47.6	0.16	21.0
Nelson R3000 Orange plate	7.54	138	42.7	0.198	51.2	0.10	19.0
Nelson R3000 Red plate	7.54	138	42.7	0.172	51.0	0.11	19.4
Nelson S3000 Purple plate	8.14	103	43.5	0.188	61.7	0.09	18.0
Senninger I-Wob Black plate	7.94	103	39.5	0.159	51.9	0.10	19.4
Group mean flow rate =			43.0				

klers may be quite different depending on soil-specific sealing characteristics, which would require detailed characterization of soil infiltration response to specific power and infiltration modeling. For sprinklers with near equal RI_g, the sprinkler with the lower ASP may have lower runoff potential on soils that seal easily, while lower AAR may be advantageous on soils with low infiltration rates and minimal soil surface sealing or protected soil surface.

The proposed sprinkler runoff index provides an effective means of comparing sprinkler choices with regard to runoff potential, despite being independent of soil characteristics, by identifying sprinklers with large droplets and relatively small wetted radii. From a practical application viewpoint, sprinklers providing RI_g values in the top 20%

of a flow rate group should all decrease potential runoff while likely having few measureable differences in runoff among them, given the degree of variability found in field infiltration rates, except perhaps where sprinkler ASP values are vastly different on easily sealing soils.

The proposed sprinkler runoff index considers only one aspect of sprinkler selection in the design of mechanical-move irrigation systems. Other factors, such as water application uniformity, wind drift, evaporation climate, soil, slope, and crops grown, need to be considered as well when selecting a sprinkler for a particular situation, as these factors also impact irrigation system performance. In climatic regions where irrigation only occurs after crop establishment, soil surface sealing by sprinkler droplet impact is of

much less concern. Actual runoff under mechanical-move irrigation is highly dependent on slope, soil surface roughness, surface cover (residue), application depth, and irrigation frequency, all of which can have a much larger impact on runoff than differences between sprinklers with regard to droplet size and wetted diameter.

CONCLUSIONS

Droplet sizes, droplet velocities, and water application rate profiles of numerous commercial mechanical-move irrigation system sprinklers were measured in the laboratory over a range of flow rates and operating pressures. Average specific power and water application rates of the sprinklers were computed by overlapping specific power and water application profiles for sprinklers equally spaced 3 m along a system lateral. A sprinkler potential runoff index independent of soil infiltration characteristics was proposed and applied to each sprinkler, flow rate, and operating pressure. The proposed sprinkler runoff index provides a new and unique approach for evaluating commercial mechanical-move irrigation sprinklers with regard to runoff potential using quantitative analysis considering application rates of kinetic energy and water from mechanical-move irrigation. The results show that substantial differences exist between sprinkler choices, and several sprinklers can have similar runoff potential index values. In some cases, equivalent potential runoff index values are obtained with compensating differences in specific power and application rate, making the selection of the best sprinkler more difficult. The sprinkler index provides an effective means for comparing sprinkler choices with regard to runoff potential by identifying sprinklers with large droplets and relatively small wetted diameters.

REFERENCES

Agassi, M., Morin, J., & Shainberg, I. (1985). Effect of raindrop impact energy and water salinity on infiltration rates of sodic soils. *SSSA J., 49*(1), 186-189. http://dx.doi.org/10.2136/sssaj1985.03615995004900010037x.

Agassi, M., Bloem, D., & Ben-Hur, M. (1994). Effect of drop energy and soil and water chemistry on infiltration and erosion. *Water Resources Res., 30*(4), 1187-1193. http://dx.doi.org/10.1029/93WR02880.

Allen, R. G. (1990). Applicator selection along center-pivots using soil infiltration parameters. In *Proc. 3rd Natl. Irrig. Symp.: Visions of the Future* (pp. 549-555). St. Joseph, Mich.: ASAE.

Assouline, S., & Mualem, Y. (1997). Modeling the dynamics of seal formation and its effect on infiltration as related to soil and rainfall characteristics. *Water Resources Res., 33*(7), 1527-1536. http://dx.doi.org/10.1029/96WR02674.

Ben-Hur, M., Shainberg, I., & Morin, J. (1987). Variability of infiltration in a field with surface-sealed soil. *SSSA J., 51*(10), 1299-1302. http://dx.doi.org/10.2136/sssaj1987.03615995005100050037x.

Ben-Hur, M., Plaut, Z., Levy, G. J., Agassi, M., & Shainberg, I. (1995). Surface runoff, uniformity of water distribution, and yield of peanut irrigated with a moving sprinkler system. *Agron. J., 87*(4), 609-613. http://dx.doi.org/10.2134/agronj1995.00021962008700040001x.

Betzalel, I., Morin, J., Benyamini, Y., Agassi, M., & Shainberg, I. (1995). Water drop energy and soil seal properties. *Soil Sci., 13*(22), 13-22. http://dx.doi.org/10.1097/00010694-199501000-00002.

Borst, H. L., & Woodburn, R. (1942). The effect of mulching and methods of cultivation on runoff and erosion from Muskingum silt loam. *Agric. Eng., 23*(1), 19-22.

Brooks, R. H., & Corey, A. T. (1964). Hydraulic properties of porous media. Hydrology Paper No. 3. Ft. Collins, Colo.: Colorado State University.

Chen, D., & Wallender, W. W. (1985). Droplet size distribution and water application with low-pressure sprinklers. *Trans. ASAE, 28*(2), 511-516. http://dx.doi.org/10.13031/2013.32288.

DeBoer, W. B., & Chu, S. T. (2001). Sprinkler technologies, soil infiltration, and runoff. *J. Irrig. Drain. Eng., 127*(4), 234-239. http://dx.doi.org/10.1061/(ASCE)0733-9437(2001)127:4(234).

DeBoer, D. W., Beck, D. L., & Bender, A. R. (1992). A field evaluation of low, medium, and high pressure sprinklers. *Trans. ASAE, 35*(4), 1185-1189. http://dx.doi.org/10.13031/2013.28718.

Duley, F. L. (1939). Surface factors affecting the rate of intake of water by soils. *SSSA J., 4*(C), 60-64. http://dx.doi.org/10.2136/sssaj1940.036159950004000C0011x.

Ellison, W. D. (1945). Some effects of rain-drops and flow on soil erosion and infiltration. *Trans. American Geophys. Union, 26*(3), 415-429.

Kincaid, D. C. (1996). Spraydrop kinetic energy from irrigation sprinklers. *Trans. ASAE, 39*(3), 847-853. http://dx.doi.org/10.13031/2013.27569.

Kincaid, D. C. (2005). Application rates from center-pivot irrigation with current sprinkler types. *Appl. Eng. Agric., 21*(4), 605-610. http://dx.doi.org/10.13031/2013.18570.

King, B. A., & Bjorneberg, D. L. (2010). Characterizing droplet kinetic energy applied by moving spray-plate center-pivot irrigation sprinklers. *Trans. ASAE, 53*(1), 137-145. http://dx.doi.org/10.13031/2013.29512.

King, B. A., & Bjorneberg, D. L. (2011). Evaluation of potential runoff and erosion of four center-pivot irrigation sprinklers. *Appl. Eng. Agric., 27*(1), 75-85. http://dx.doi.org/10.13031/2013.36226.

King, B. A., & Bjorneberg, D. L. (2012a). Transient soil surface sealing and infiltration model for bare soil under droplet impact. *Trans. ASABE, 55*(3), 937-945. http://dx.doi.org/10.13031/2013.41525.

King, B. A., & Bjorneberg, D. L. (2012b). Droplet kinetic energy of moving spray-plate center-pivot irrigation sprinklers. *Trans. ASABE, 55*(2), 505-512. http://dx.doi.org/10.13031/2013.41386.

King, B. A., Winward, T. W., & Bjorneberg, D. L. (2010). Laser precipitation monitor for measurement of drop size and velocity of moving spray-plate sprinklers. *Appl. Eng. Agric., 26*(2), 263-271. http://dx.doi.org/10.13031/2013.29551.

McIntyre, D. S. (1958). Permeability measurements of soil crusts formed by raindrop impact. *Soil Sci., 85*(4), 185-189. http://dx.doi.org/10.1097/00010694-195804000-00002.

Mohammed, D., & Kohl, R. A. (1987). Infiltration response to kinetic energy. *Trans. ASAE, 30*(1), 108-111. http://dx.doi.org/10.13031/2013.30410.

Nash, J. E., & Sutcliffe, J. V. (1970). River flow forecasting through conceptual models: Part 1. A discussion of prinicples. *J. Hydrol., 10*(3), 282-290. http://dx.doi.org/10.1016/0022-1694(70)90255-6.

Ogden, C. B., van Es, H. M., & Schindelbeck, R. R. (1997). Miniature rainfall simulator for field measurement of soil infiltration. *SSSA J., 61*(4), 1041-1043. http://dx.doi.org/10.2136/sssaj1997.03615995006100040008x.

Saxton, K. E., & Rawls, W. J. (2006). Soil water characteristics

estimates by texture and organic matter for hydrologic solutions. *SSSA J., 70*(5), 1569-1578. http://dx.doi.org/10.2136/sssaj2005.0117.

Silva, L. L. (2006). The effect of spray head sprinklers with different deflector plates on irrigation uniformity, runoff, and sediment yield in a Mediterranean soil. *Agric. Water Mgmt., 85*(3), 243-252. http://dx.doi.org/10.1016/j.agwat.2006.05.006.

Thompson, A. L., & James, L. G. (1985). Water droplet impact and its effect on infiltration. *Trans. ASAE, 28*(5), 1506-1510. http://dx.doi.org/10.13031/2013.32468.

Undersander, D. J., Marek, T. H., & Clark, R. N. (1985). Effect of nozzle type on runoff and yield of corn and sorghum under center-pivot sprinkler systems. *Irrig. Sci., 6*(1), 107-116. http://dx.doi.org/10.1007/BF00251559.

USDA. (2014). 2013 Farm and ranch irrigation survey. Washington, D.C.: USDA National Agricultural Statistics Service. Retrieved from www.agcensus.usda.gov/Publications/2012/Online_Resources/Farm_and_Ranch_Irrigation_Survey/.

von Bernuth, R. D., & Gilley, J. R. (1985). Evaluation of center-pivot application packages considering droplet-induced infiltration reduction. *Trans. ASAE, 28*(6), 1940-1946. http://dx.doi.org/10.13031/2013.32545.